J. Membrane Biol. 132, 157–166 (1993)

The Journal of
Membrane Biology

Ca^{2+} Transport across Intestinal Brush Border Membranes of the Cichlid Teleost *Oreochromis mossambicus*

Peter H.M. Klaren, Gert Flik, Robert A.C. Lock, and Sjoerd E. Wendelaar Bonga
Department of Animal Physiology, Faculty of Science, University of Nijmegen, 6525 ED Nijmegen, The Netherlands

Summary. Brush border membranes were isolated from tilapia (*Oreochromis mossambicus*) intestine by the use of magnesium precipitation and differential centrifugation. The membrane preparation was enriched 17-fold in alkaline phosphatase. The membranes were 99% right-side-out oriented as indicated by the unmasking of latent glyceraldehyde-3-phosphate dehydrogenase and acetylcholine esterase activity by detergent treatment.

The transport of Ca^{2+} in brush border membrane vesicles was analyzed. A saturable and a nonsaturable component in the uptake of Ca^{2+} was resolved. The saturable component is characterized by a K_m much lower than the Ca^{2+} concentrations predicted to occur in the intestinal lumen. The nonsaturable component displays a Ca^{2+} permeability too high to be explained by simple diffusion. We discuss the role of the saturable component as the rate-limiting step in transmembrane Ca^{2+} movement, and suggest that the nonsaturable component reflects a transport mechanism operating well below its level of saturation.

Key Words Ca^{2+} transport · brush border membrane · enterocyte · fish intestine · tilapia

Introduction

In freshwater fish, the gills are are the major site for Ca^{2+} uptake from the (hypocalcic) water environment [8, 41]. In combined in vivo and in vitro studies Flik et al. [10, 12, 13] identified a high-affinity Ca^{2+}-ATPase as the pivotal mechanism in active Ca^{2+} transport in the gills of freshwater tilapia (*Oreochromis mossambicus* Peters) and North-American eel (*Anguilla rostrata* LeSueur).

Uptake of calcium via the intestine provides a second important pathway. Indeed, Berg [1], Dacke [4] and Ichii and Mugiya [22] described important contributions of dietary calcium to the total Ca^{2+} uptake in fish. The prevailing intracellular Ca^{2+} concentrations ($\approx$80 nmol · l^{-1}) are nonsaturating for the basolateral Ca^{2+} extruding mechanisms [11, 34]. The rate-limiting step of transepithelial Ca^{2+} transport therefore seems to be the Ca^{2+} entry at the apical membrane. The primary site of hormonal control of Ca^{2+} uptake has been suggested to be in the apical membrane of cells in the gills and intestine [25, 30]. In tilapia, transepithelial Ca^{2+} transport is sodium dependent and associated with a powerful Na^+/Ca^{2+} exchanger. Furthermore, the enterocyte is equipped with a high-affinity ATP-dependent Ca^{2+} transporter [11, 34].

In fish, at least in some species, the calcium metabolism is hormonally controlled by prolactin or cortisol that exert hypercalcemic effects, and by the hypocalcemic hormone stanniocalcin (STC) [44]. STC is produced in the corpuscles of Stannius, unique for teleost fish. Besides the uptake of Ca^{2+} in the gills, STC is also involved in the intestinal uptake of Ca^{2+} in freshwater and seawater fish. Hirano [19] reported an increased Ca^{2+} absorption in intestine from freshwater-adapted eel in which the corpuscles of Stannius were surgically removed.

The fish enterocyte provides a unique model with defined endocrine control mechanisms at the apex and basis of the cell. The aim of this study was to analyze the Ca^{2+} transporting mechanism in the apical membrane of the tilapia enterocyte.

Materials and Methods

Sexually mature tilapia (*Oreochromis mossambicus*) of both sexes, obtained from laboratory stock and weighing 250 to 450 g, were kept in 100-liter aquaria, supplied with running Nijmegen tap water (8–10 mOsmol, $[Ca^{2+}]$ = 0.8 mmol · l^{-1}, 25°C) under a photoperiod of 16 hr light : 8 hr darkness. The fish were fed Trouvit® commercial fish food (Trouw, Putten, The Netherlands), 1.5% of the body weight per day.

Materials

$^{45}CaCl_2$ and D-[1-^{14}C]mannitol were purchased from Amersham (UK). Trizma-7.0® and Scintillator 299™ were from Sigma® (no. T 3503) and Packard, respectively. All other chemicals were analytical grade and obtained from commercial suppliers.

Table. Enrichment and relative recoveries of marker enzyme activities in tilapia intestinal brush border membrane preparations (mean ± SEM)

Marker	Enrichment[a]	Recovery[b] (%)	n
APase[c]	17.0 ± 3.2	5.1 ± 0.8	9
$(Na^+ + K^+)$-ATPase	2.8 ± 0.5	0.9 ± 0.2	11
SDH	0.15 ± 0.07	0.06 ± 0.03	6
β-D-Glucuronidase	0.7 ± 0.1	0.30 ± 0.04	6
Protein		0.32 ± 0.02	12

[a] Enrichment is the ratio of the specific activities in the brush border membrane preparation and in the initial homogenate.
[b] Recovery was calculated as the percentage total activity (equals specific activity × total protein) in the brush border membrane preparation relative to that in the initial homogenate.
[c] The activity of sucrase, another brush border membrane marker, was not detectable in the initial homogenate. In eight brush border membrane preparations the specific sucrase activity averaged 4.0 ± 0.4 μmol glucose · hr^{-1} · mg^{-1} (mean ± SEM).

Isolation of Intestinal Brush Border Membranes

Fish were killed by spinal transection. The peritoneal cavity was opened and the intestinal tract exposed. All subsequent steps were performed at 0–4°C. The proximal 30 cm of the intestine were quickly removed, flushed with ice-cold saline containing 150 mmol · l^{-1} NaCl, 1 mmol · l^{-1} N-[2-hydroxethyl]piperazine-N′-[2-ethanesulphonic acid] (HEPES)/Tris(hydroxy-methyl) aminomethane (Tris), pH 8.0, 1 mmol · l^{-1} dithiothreitol and 0.1 mmol · l^{-1} ethylene-diaminetetraacetic acid (EDTA), cut open lengthwise and rinsed with the same saline. The mucosa was scraped off its underlying muscle layers with the aid of a microscope slide. From one fish, around 0.6 g wet weight scrapings were obtained. Scrapings were disrupted by 25 strokes in a glass dounce homogenizer equipped with a loosely fitting pestle in 40 ml homogenization buffer containing 250 mmol · l^{-1} sucrose, 10 mmol · l^{-1} HEPES/Tris, pH 8.0, 1 mmol · l^{-1} dithiothreitol, and 100 U · ml^{-1} of the proteinase inhibitor aprotinine. This homogenate was centrifuged for 10 min at 1,400 × g. The resulting supernatant (containing about 70% of the total $(Na^+ + K^+)$-ATPase activity present in the initial homogenate) was discarded. The pellet, which contains the brush border membranes, was resuspended in 40 ml homogenization buffer by 25 strokes in a glass dounce homogenizer and centrifuged for 20 min at 1,400 × g as described above. With the resulting supernatant, an additional 20% of the total $(Na^+ + K^+)$-ATPase activity was removed. The pellet was resuspended in 5 ml mannitol buffer containing 300 mmol · l^{-1} mannitol, 12 mmol · l^{-1} Tris/HCl, pH 7.1, using a glass dounce homogenizer (3–7 strokes) and passed through cheesecloth. Five volumes of ultrapure water were added to this suspension and the mixture was homogenized by 20 strokes in a glass dounce homogenizer. Solid $MgCl_2$ was added to obtain a final concentration of 10 mmol · l^{-1}, and the suspension was mildly agitated for 15 min. To collect the brush border membranes, the suspension was centrifuged (3,000 × g, 15 min); the resulting supernatant was spun at 27,000 × g, 30 min. The pellet, containing the brush border membranes, was resuspended by 30 passages through a 23–G needle and collected in 10 ml KCl buffer containing 150 mmol · l^{-1} KCl, 0.8 mmol · l^{-1} free Mg^{2+} and 20 mmol · l^{-1} HEPES/Tris, pH 7.4. Depending on the subsequent assay to be performed, the required amounts of $CaCl_2$, ethylene glycol-bis-(β-aminoethyl ether) (EGTA), N-(2-hydroxyethyl)-ethylenediamine-N′,N,N′-triacetic acid (HEEDTA) and nitrilotriacetic acid (NTA) were added to this KCl buffer, thus allowing loading of the vesicles with the substances mentioned. Finally, the brush border membranes were pelleted by centrifuging at 27,000 × g, 60 min, and resuspended by 30 passages through a 23–G needle in 0.2–0.4 ml assay buffer. The total isolation procedure lasted 4–5 hr, experiments started within 3 hr after isolation.

Enzyme Assays

Protein recovery was 0.32 ± 0.02% (mean ± SEM, n = 12). The membrane preparations contained 0.4–0.8 mg · ml^{-1} protein and were used on the day of isolation. The marker enzymes used to characterize the membrane preparation were: alkaline phosphatase (APase, EC 3.1.3.1) and sucrase (EC 3.2.1.48) for brush border membranes, $(Na^+ + K^+)$-ATPase (EC 3.6.1.3) for basolateral membranes, succinate dehydrogenase (SDH, EC 1.3.99.1) for mitochondria, and β-D-glucuronidase (EC 3.2.1.31) for lysosomes. Assay procedures for APase, $(Na^+ + K^+)$-ATPase and SDH have been described by Flik et al. [12]. The sucrase and β-D-glucuronidase activities were assayed according to Dahlqvist [5] and Fishman and Bernfeld [9], respectively. Membrane protein content was determined with a commercial Coomassie Brilliant Blue reagent kit (Biorad), using bovine serum albumin as a reference. Membranes were preincubated with 0.4 mg saponin per mg membrane protein to permeabilize membrane vesicles and to maximize enzyme activity. Data on purification and recovery of marker enzymes are presented in the Table. The brush border membrane preparation is enriched in sucrase and 17-fold in APase. Membranes are not contaminated with mitochondria and lysosomes, and only slightly with basolateral membranes. The specific APase activity averaged 339.3 ± 34.9 μmol nitrophenol · hr^{-1} · mg^{-1} (mean ± SEM, n = 9), measured at 37°C, pH 10.4. The values for purification and recovery are congruent with those presented by Pelletier et al. [29] who isolated brush border membranes from trout intestine using a calcium precipitation technique. Their values for the specific APase activity, however, are two orders of magnitude lower than those reported here. Titus et al. [42] isolated brush border mem-

branes from tilapia intestine using a comparable procedure. They reported a similar APase enrichment of their preparation as in the present study.

Intravesicular Space and Membrane Orientation

Intravesicular space was determined according to Flik et al. [11]. Membrane vesicles (collected in KCl buffer) were equilibrated for 2 hr at 37°C in KCl buffer, containing 0.1 mmol · l^{-1} D-mannitol and labeled with 161 kBq · ml^{-1} D-[1-^{14}C]mannitol. The intravesicular space of the brush border membrane vesicles (BBMV), calculated from the equilibrium mannitol content, was 6.0 ± 1.5 μl · mg^{-1} protein (n = 6). The percentage of right-side-out oriented vesicles was determined on the basis of latent glyceraldehyde-3-phosphate dehydrogenase (EC 1.2.1.12) activity using D-glyceraldehyde-3-phosphate as a substrate. The percentage of inside-out oriented vesicles was determined on the basis of latent acetylcholine esterase (EC 3.1.1.7) activity, using acetylthiocholine as a substrate. Procedures were according to Steck and Kant [37]. Unmasking of latent enzyme activity by Triton X-100 treatment revealed 99.0 ± 1.3% right-side-out oriented vesicles, and 7.6 ± 5.2% inside-out oriented vesicles (mean values ± SD, n = 4). The high percentage of resealed right-side-out BBMV is consistent with the observations on rat small intestinal BBMV by Haase et al. [17].

Vesicle Ca^{2+} Transport

Two approaches were followed to study Ca^{2+} transport across brush border membranes, *viz.* (i) zero *trans* uptake and (ii) isotope equilibrium exchange. A rapid filtration technique was used to determine Ca^{2+} content of BBMV. All transport studies were performed in duplicate, blank values were determined in quadruplicate.

Zero Trans Studies

In zero *trans* uptake studies, Ca^{2+} transport is measured in Ca^{2+}-free BBMV. Time course analysis and kinetic studies of the initial rate of Ca^{2+} uptake were performed.

Membrane vesicles were collected in Ca^{2+}-free KCl buffer. The assay medium consisted of KCl buffer, to which had been added 0.01 to 5 mmol · l^{-1} free Ca^{2+}, 0.5 mmol · l^{-1} EGTA, 0.5 mmol · l^{-1} HEEDTA and 0.5 mmol · l^{-1} NTA. The concentration $^{45}Ca^{2+}$ (added as $^{45}CaCl_2$) in the assay medium was 0.8–1.0 MBq · ml^{-1}. Incubations were carried out at 37°C, membranes and assay medium were prewarmed before incubation. Samples, containing 50 μl of the incubate, were quenched in 1 ml ice-cold stop buffer (containing 150 mmol · l^{-1} KCl, 20 mmol · l^{-1} Trizma-7.0®, pH 7.4, and 1.0 mmol · l^{-1} EGTA) The quenched sample was immediately filtered over an 80-kPa vacuum (Schleicher & Schüll ME25 nitrocellulose filters, pore size 0.45 μm). The filters were rinsed three times with 2 ml of ice-cold stop buffer and dissolved in 4 ml of Scintillator 299™ scintillation fluid. The radioactivity of the filters was determined in a Wallac 1410 liquid scintillation counter. Blank values were obtained by incubating vesicles at 0°C, immediately followed by sampling, quenching and filtering as described above. Calcium uptake values are corrected by subtracting blank values and are expressed as nmol · sec^{-1} per mg protein. When uptakes were measured at time intervals shorter than 10 sec, an automated stopped-flow apparatus was used.

Isotope Equilibrium Exchange

In isotope equilibrium exchange experiments no net flux of substrate occurs. Instead, the distribution rate of the tracer $^{45}Ca^{2+}$ under equilibrium conditions, i.e., when there is no electrical potential and the *cis* and *trans* $^{40}Ca^{2+}$-concentrations are equal, is measured. Isotope exchange across the membrane is therefore exponential.

Equilibrium Exchange Influx

Membrane vesicles were resuspended in (tracer-free) assay buffer before the last centrifugation step. The same buffer as in the zero *trans* experiments was used. All subsequent steps of the isolation procedure were then performed in the same assay buffer, thus allowing loading of the vesicles with Ca^{2+}. To measure isotope exchange, membrane vesicles were diluted in the same assay buffer to which 0.8–1.0 MBq · ml^{-1} $^{45}Ca^{2+}$ was added. The stop buffer contained 150 mmol · l^{-1} KCl, 20 mmol · l^{-1} Trizma-7.0®, pH 7.4, and a concentration La^{3+} at least two times higher than the concentration of free Ca^{2+} in the assay medium. Blanks and samples were prepared as described for the zero *trans* experiments. The $^{45}Ca^{2+}$ content of the membrane vesicles is expressed in dpm per mg membrane protein. Data are corrected by subtracting the blank value from the exchange values.

Equilibrium Exchange Efflux

After 21 min (more than 8 × $t_{1/2}$ for isotope exchange influx) 150 μl of the incubate was diluted in 2 ml of (prewarmed) assay buffer, containing $^{40}Ca^{2+}$ only. When diluted, the vesicles contained approximately 5% of the total radioactivity content in the assay medium. The $^{45}Ca^{2+}$ concentration in the vesicles was then 30 times higher than in the medium surrounding the vesicles. An isotope exchange in an essentially isotope-free medium is thus measured. Samples (0.4 ml) from this mixture were quenched in 2 ml stop buffer and immediately filtered. Filters were rinsed, dissolved and the radioactivity counted as described above. Experimentally it was not feasible to obtain true blank values, i.e., measurements of the vesicle tracer content at time point zero, for the equilibrium isotope efflux exchange. These data are therefore presented without zero point correction.

Effectiveness of the Loading Procedure and Quenching

Membrane vesicles were allowed to load $^{40}Ca^{2+}$ and $^{45}Ca^{2+}$ in an assay buffer that contained 5.0 mmol · l^{-1} $^{40}Ca^{2+}$ and 60 kBq · ml^{-1} $^{45}Ca^{2+}$. After loading, vesicles were diluted in the same assay medium, sampled, quenched and filtered immediately. In a control experiment, vesicles from the same membrane preparation were loaded with $^{40}Ca^{2+}$ only and incubated for 30 min in a medium with the same specific activity. Vesicles from the control experiment were compared with the $^{40}Ca^{2+}$ and $^{45}Ca^{2+}$ loaded vesicles; the tracer content of the last mentioned was calculated to be 105.2 ± 6.5% (mean ± SD, n = 5) of the control vesicles.

Thus, the loading procedure was effective, and our assumption of an equilibrium condition with respect to calcium justified.

Samples, containing 150 μl from the control incubation, were also quenched in 3 ml ice-cold stop buffer containing 10 mmol · l^{-1} La^{3+} or 1.0 mmol · l^{-1} EGTA. Immediately after quenching, as well as two and five minutes thereafter, aliquots of a quenched sample were filtered and analyzed for radioactivity content. No significant decrease of vesicle $^{45}Ca^{2+}$ content with time was found. The use of lanthanum and EGTA as agents to stop Ca^{2+} movements was thus appropriate.

Calculations and Statistics

Free Ca^{2+} and Mg^{2+} concentrations were calculated according to Schoenmakers et al. [35], using the computer program CHELATOR which allows correcting metal-chelator stability constants for effects of temperature, ionic strength and proton activity of the medium. The first and second protonations of the chelating compounds were taken into account. Stability constants are from Sillén and Martell [36].

The (initial) Ca^{2+}-dependent zero *trans* Ca^{2+}-uptake could be described by a function containing a saturable and a non-saturable term:

$$J = \frac{J_{max} \times [S]}{K_m + [S]} + c \times [S] \quad (1)$$

where $[S]$ stands for the free Ca^{2+} concentration in the medium, J_{max} represents the limiting flux (i.e., at infinitely high $[S]$), K_m is the substrate concentration at which J is half maximal, and c is a constant having the dimension of a limiting permeability (i.e., J_{max}/K_m). Data from isotope equilibrium exchange influx and efflux experiments were fitted to the exponential equations (2) and (3), respectively:

$$f(t) = A_1 \cdot (1 - \exp(-k_1 t)) + A_2 \cdot (1 - \exp(-k_2 t)) \quad (2)$$

$$f(t) = A \cdot \exp(-kt) + \text{Offset} \quad (3)$$

where A represents the limit of a component (i.e., $^{45}Ca^{2+}$-counts per mg protein) and k is a first-order rate constant. The offset represents the tracer content (adsorbed and exchanged tracer) of the BBMV. Subscripts specify parameters of two exponents. Effects of a nonhomogeneity of the BBMV population (i.e., vesicle size, functionally different vesicle subpopulations) on equilibrium exchange influxes and effluxes were analyzed using Hopfer's [21] criteria. Accordingly, k_i, the rate constant for an individual vesicle i, is considered as the product of the rate constant r of a transporter common in all vesicles, and a "lumped" constant h_i, including the contribution of the area-to-volume-ratio (i.e., vesicle size) of an individual vesicle i to the actual isotope exchange influx and efflux determined. Then, $k_i = h_i \cdot r$, and Eqs. (2) and (3) transform to:

$$f(t) = \Sigma\, w_i \cdot \exp(-h_i r t), \quad (4)$$

in which w_i weights the contribution of vesicle i to the actual macroscopic isotope exchange measured. The transporter's rate constant r is dependent on experimental variables such as substrate concentration and temperature, whereas the constant h_i varies only with vesicle size, transporter density and other vesicle specific parameters. Hopfer [21] then showed that, by defining normalized time $\tau = r \cdot t_{1/2}$ ($\propto t/t_{1/2}$), Eq. (4) becomes

$$f(\tau) = \Sigma\, w_i \cdot \exp(-h_i \tau), \quad (5)$$

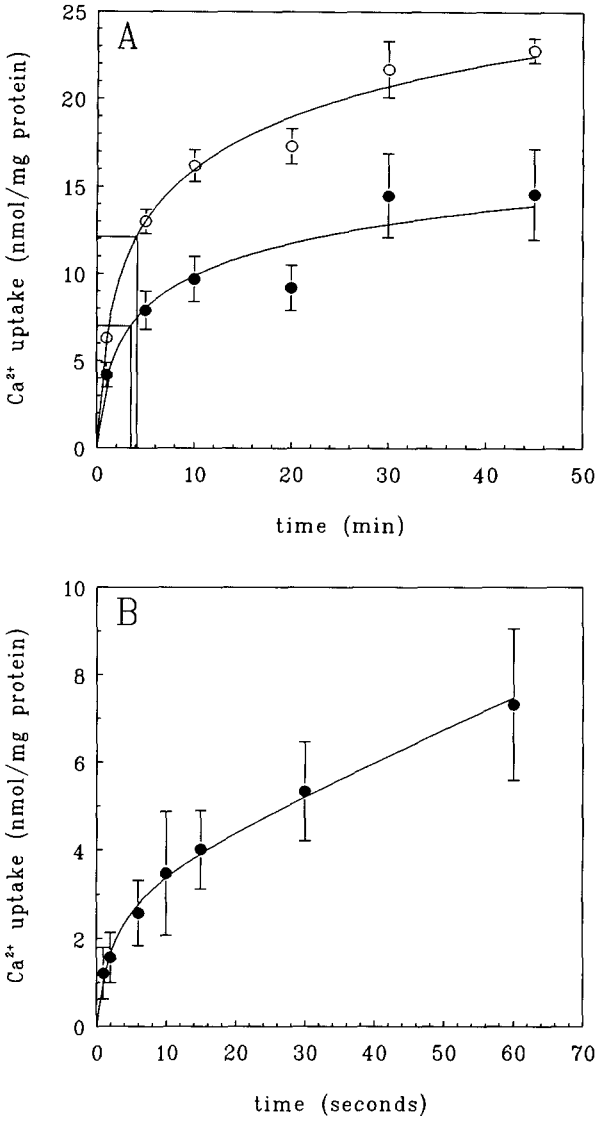

Fig. 1. Time course of zero *trans* Ca^{2+} uptake in BBMV. Means and SEM are shown. (*A*) Filled circles: 0.5 mmol · l^{-1} Ca^{2+} (n = 7); open circles: 5.0 mmol · l^{-1} Ca^{2+} (n = 4). (*B*) Uptake at 0.5 mmol · l^{-1} Ca^{2+} during the first minute of the incubation (n = 5).

describing the time dependence of isotope exchange as a function of an experimental variable which affects the transporter's activity.

Data were analyzed using a nonlinear regression data analysis program [24]. Student's t-test was used for statistical evaluation. Significance was accepted for $P < 0.05$.

Results

Time course studies of zero *trans* calcium uptake by BBMV are shown in Fig. 1*A* and *B*. The uptake of Ca^{2+} in BBMV in the presence of 0.5 mmol · l^{-1} Ca^{2+} plateaued after 10 min. On the basis of the equilibrium Ca^{2+} content we calculate a vesicular volume of 7.7 ± 1.8 μl · mg^{-1} protein (mean ± SD),

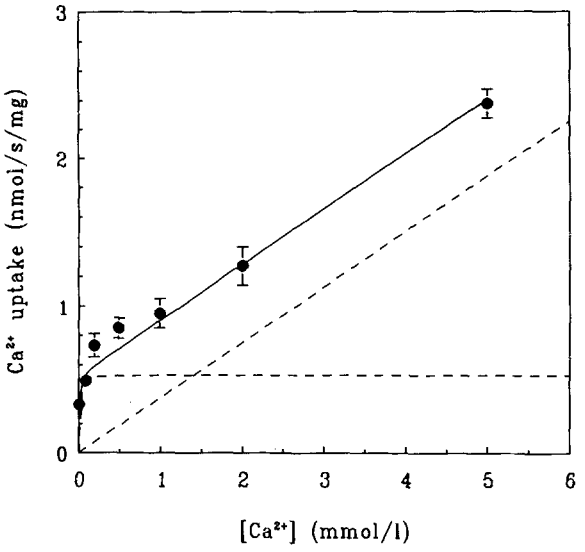

Fig. 2. Ca^{2+}-dependent Ca^{2+} uptake in BBMV. Uptake was measured during 1-sec incubations. Mean values and SEM for five different membrane preparations are given. The Ca^{2+} concentration in the assay medium was varied from 10 μmol · l^{-1} to 5 mmol · l^{-1}. Data points were fitted to Eq. (1). Estimates of kinetic parameters are: J_{max} = 0.53 nmol Ca^{2+} · mg^{-1} · sec^{-1}, K_m = 5.8 μmol · l^{-1} Ca^{2+}, c = 376 nl · sec^{-1} · mg^{-1}. Dotted lines indicate the saturable and nonsaturable component from Eq. (1).

which is not significantly different from the vesicular mannitol space of 6.0 ± 1.5 μl · mg^{-1} protein. Obviously the blank value is a proper representation of tracer binding to the vesicle interior and exterior. Zero *trans* Ca^{2+} uptake deviates fast from linearity, and is linear only during the first second of the time course (Fig. 1*B*). Figure 1*A* also shows the uptake in the presence of 5.0 mmol · l^{-1} Ca^{2+} in the extravesicular medium. From the two curves describing the time courses of the zero *trans* uptake at two Ca^{2+} concentrations a similar half-time value of 4 min is obtained.

Figure 2 shows the Ca^{2+} dependent zero *trans* Ca^{2+} uptake in BBMV at initial rate. A saturable and a nonsaturable, linear component can be distinguished. The saturable component is described by a Michaelis-Menten equation. The kinetic parameters J_{max} and K_m were calculated to be 0.53 nmol · sec^{-1} · mg^{-1}, and 5.8 μmol · l^{-1} Ca^{2+}, respectively. The constant c in the nonsaturable term $c \times [S]$ of Eq. (1) is calculated to be 376 nl · sec^{-1} · mg^{-1}. From the intersection of the curves describing the saturable and nonsaturable component the $[Ca^{2+}]$ at which both components contribute equally to the total uptake can be obtained. Figure 2 demonstrates this to be 1.5 mmol · l^{-1}.

Figure 3*A* and *B* show the results of equilibrium isotope influxes and effluxes. Data could not be fitted to a single exponential, indicating a heterogeneity of the BBMV population with respect to vesicle

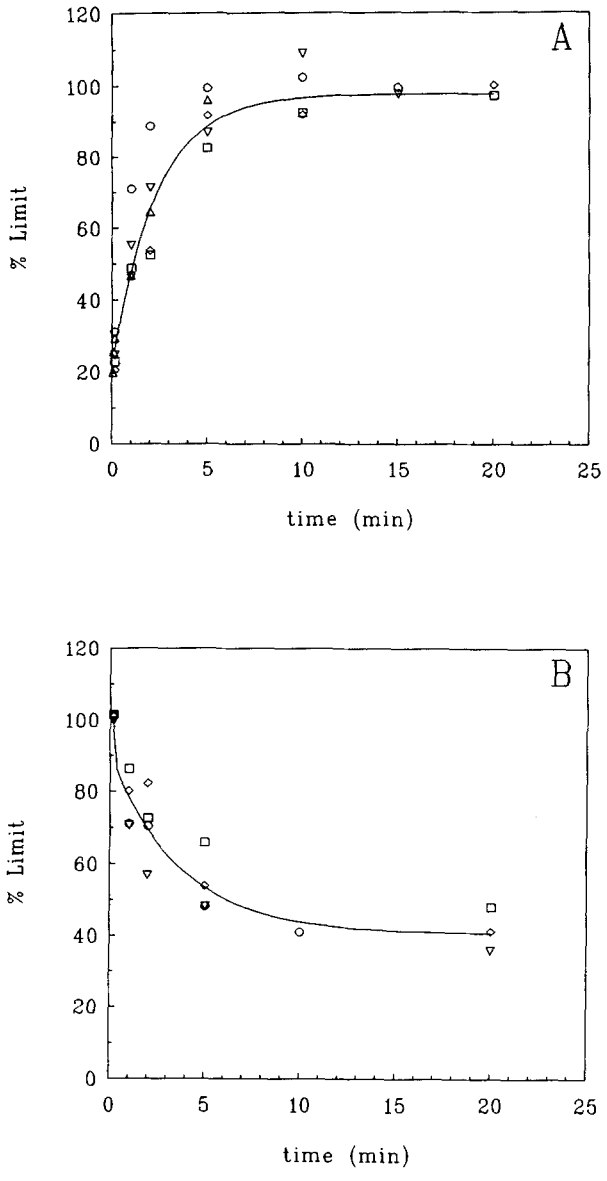

Fig. 3. Equilibrium $^{45}Ca^{2+}$ exchange data. Isotope influxes (*A*) and effluxes (*3B*) are shown. Exchange data were fitted to Eqs. (2) and (3). The tracer content of the BBMV is expressed as the percentage of the amplitude (limit) of the exponential equation describing tracer exchange. Mean values for at least four different membrane preparations are given. The following Ca^{2+} concentrations (in mmol · l^{-1}) were tested (numbers in parentheses indicate n for influx and efflux experiments, respectively): △ 0.1 (6); ○ 0.5 (7, 7); ▽ 1.0 (6, 8); □ 5.0 (5, 6); ◇ 10.0 (4, 4).

size, functional differences of the calcium transporter, or both. Moreover, there is a considerable scattering of the data around a curve of best fit. The half-time values for influx and efflux experiments are estimated to be 0.6 and 2.0 min, respectively. The rate of D-[1-^{14}C]mannitol equilibrium exchange (shown in Fig. 4*A* and *B*) is slower than the $^{45}Ca^{2+}$ exchange rate. Due to the slower rate of exchange, D-[1-^{14}C]mannitol movements are more accurately

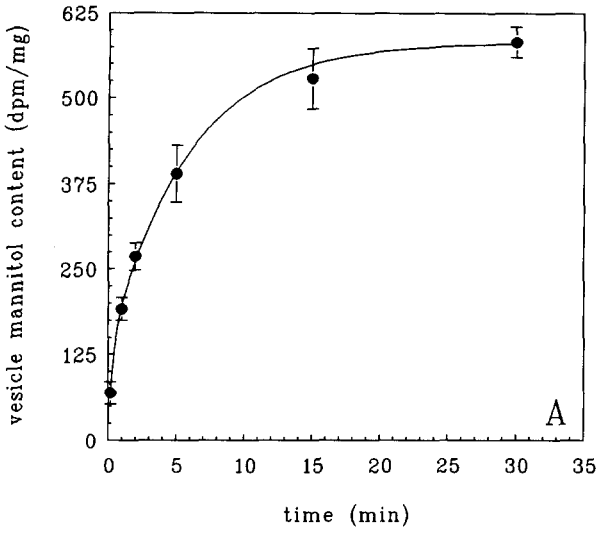

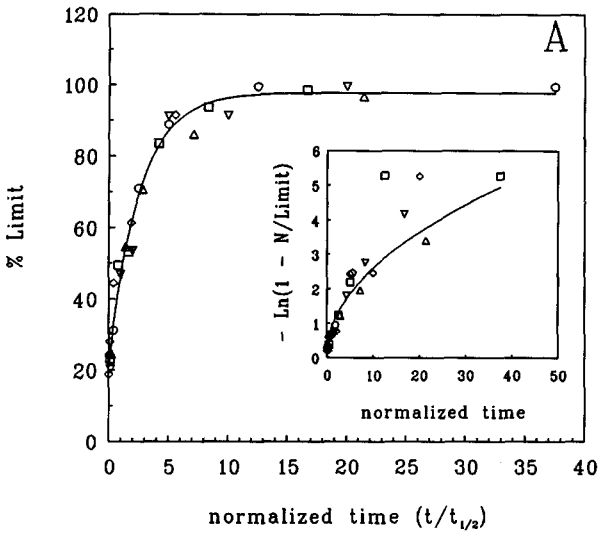

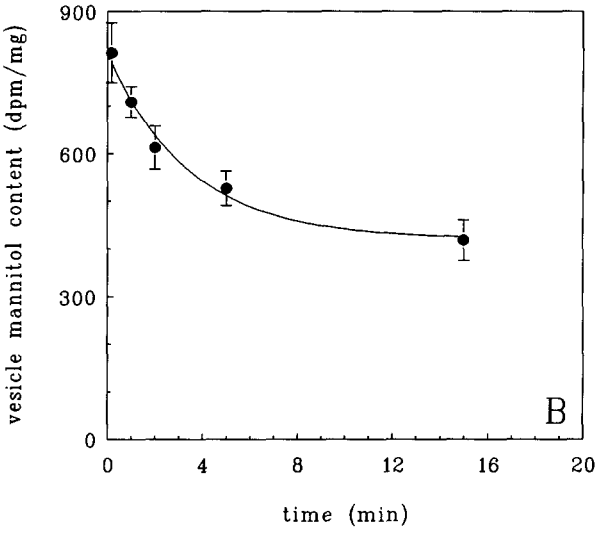

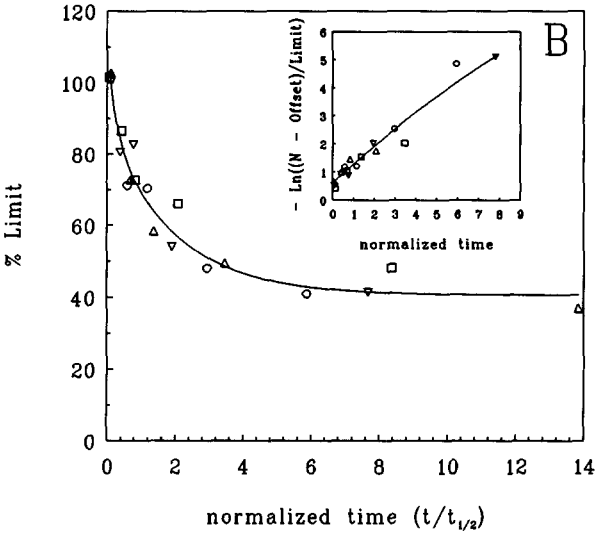

Fig. 4. Equilibrium D-[1-^{14}C]mannitol exchange data. Mean values and SEM of tracer influxes (*A*) and effluxes (*B*) for four different membrane preparations are shown. Membrane vesicles were loaded with 1.5 mmol · l^{-1} D-mannitol the same way as described for Ca^{2+}. Assay conditions were the same as for the determination of intravesicular space. Half-time values are 2.4 and 2.3 min for influx and efflux, respectively.

Fig. 5. Equilibrium $^{45}Ca^{2+}$ exchange data. Isotope influxes (*A*) and effluxes (*B*) are shown. The tracer content of the BBMV (expressed as a percentage of the amplitude of the exponential function describing tracer exchange) is shown as a function of normalized time (τ). The inset of the graphs shows ln-transformations of the data. In general, isotope exchange is described by a function of the type $f(t) = \Sigma\, w_i \cdot \exp(-h_i rt)$.

measured and, hence, the rates of exchange influx and efflux are more reliably estimated. Figure 4*A* and *B* show the half-time values for D-[1-^{14}C]mannitol exchange influx and efflux to be 2.4 and 2.3 min, respectively. The similarity of these exchange rates validates our assumption of true equilibrium conditions in our experimental setup.

As is shown in Fig. 5*A* and *B*, plotting equilibrium exchange data as a function of normalized time τ reduces the scattering. Data points are now conveniently described by a single curve. This indicates that the BBMV population consists of "similar" [21] vesicles, i.e., vesicles differing in size or transporter density only. More importantly, the process of equilibrium exchange, measured over a range of 0.1 to 10 mmol · l^{-1} Ca^{2+}, does not show saturation. The lack of a correlation between the exchange rate and the substrate concentration is indicative of a

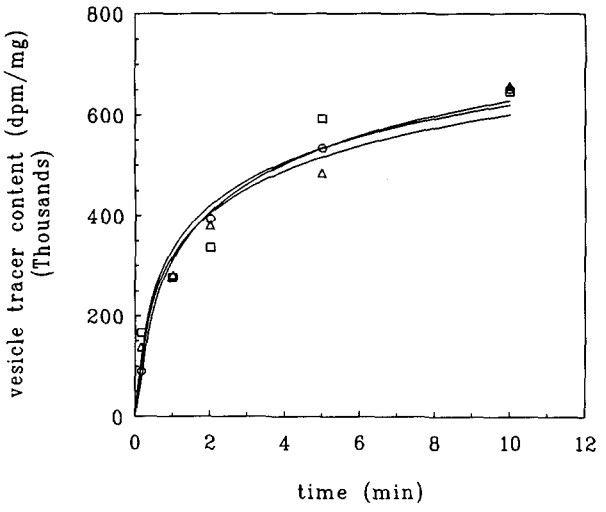

Fig. 6. Effect of external osmolarity on $^{45}Ca^{2+}$ equilibrium influx in BBMV. During the final isolation steps, BBMV were homogenized and collected in 100 mOsmol lactose and 5.0 mmol · l^{-1} Ca^{2+}. Membrane vesicles were incubated in uptake media containing sufficient lactose to reach the indicated osmolarity. Other assay conditions are the same as for equilibrium exchange, as described in Materials and Methods. (○ 152 mOsmol, □ 253 mOsmol, △ 286 mOsmol).

passive diffusion process or for the activity of a transporter operating well below its level of saturation.

The rate constant of exchange is directly proportional to the surface area of a vesicle and the permeability of a membrane, and inversely proportional to the vesicle's volume. A check for passive diffusion of a substrate can then be performed by measuring substrate uptake in vesicles with different area-to-volume ratios. Figure 6 shows equilibrium influxes in BBMV, measured at increasing osmolarities of the extravesicular medium. Influx curves are superimposable for all conditions employed. Any change in vesicular volume would have been indicated by different exchange rates and different limits of the curves describing these tracer exchanges. The BBMV do not behave as osmometers, i.e., they do not shrink predictably as a response to an increase in external osmolarity.

Discussion

The Ca^{2+}-dependent zero *trans* uptake in tilapia intestinal BBMV is a curvilinear process. Similar kinetics for Ca^{2+} uptake were observed in BBMV of hamster duodenum and ileum [23, 32], rat small intestine [14, 18, 26, 33, 45], chick duodenum [31] and human small intestine [15]. In general curvilinear patterns for the uptake of electrolytes as well as nonelectrolytes are found. This was shown to be the case for e.g., the uptake of Zn^{2+} in BBMV from pig small intestine [40], and the uptake of acetate, D-glucose and L-proline in tilapia BBMV [42]. Since a curvilinear uptake is displayed by many hydrophilic solutes [3], this does not seem to be a specific property of brush border membranes.

In stripped intestinal mucosa from tilapia, and in the presence of 1.25 mmol · l^{-1} Ca^{2+} on the mucosal side of the preparation, a net transepithelial Ca^{2+} flux of 34 ± 8 nmol · hr^{-1} · cm^{-2} was measured [11]. From the intravesicular volume of 7.7 μl · mg^{-1} for BBMV, a vesicle membrane area of 18.9 μm^2 · mg^{-1} is calculated. Assuming that the luminal area represents brush border membrane, 1 cm^2 of intestinal lumen is then equivalent to 529 mg brush border membrane protein. The net transepithelial flux, as measured by Flik et al. [11], can then be expressed as 5 nmol Ca^{2+} · sec^{-1} · mg^{-1}. Figure 2 shows the uptake in BBMV at 1.25 mmol · l^{-1} Ca^{2+} to be 1 nmol Ca^{2+} · sec^{-1} · mg^{-1}, five times lower than the net transepithelial flux. Such a difference can be anticipated, considering the folding of the lumen and the presence of intestinal microvilli in tilapia.

Zero *trans* uptakes can be biased by binding of Ca^{2+} to charged membrane surface areas [21, 43]. This can result in a virtually Ca^{2+}-deplete intravesicular medium, and hence an artificial prolonged linear phase in the transmembrane movement of Ca^{2+}. From the uptake of Ca^{2+} and mannitol into BBMV we concluded that Ca^{2+} binding to the vesicle interior and exterior was appropriately corrected for. Therefore, our measurements seem to represent true initial uptake rates. The curvilinearity of the Ca^{2+}-dependent uptake in BBMV is usually explained by the presence of a saturable (or channel- or carrier-mediated) component and a nonsaturable (or diffusional) component. Many investigators have focused on the saturable component only, which is considered to be the regulated mechanism in brush border membrane Ca^{2+} entry. We obtained a Ca^{2+} concentration of 1.5 mmol · l^{-1} at which the contribution of each component to the total Ca^{2+} uptake is equal. Luminal Ca^{2+} concentrations are in the range of 5–25 mmol · l^{-1} (*personal observation*). The saturable component is then operating under J_{max} conditions, and, having a K_m in the micromolar range, is obviously not the rate-limiting step in brush border membrane transport. The question then arises whether the nonsaturable component is rate limiting and whether this is a true diffusion process. Indeed, Christensen [3] suggested that an apparently linear portion of a curve describing uptake rate as a function of substrate concentration could well be a part of a second rec-

tangular hyperbola characterizing a second saturable component.

Information on the nonsaturable component is contained in the constant c of Eq. (1), for tilapia BBMV calculated to be 376 nl · sec^{-1} · mg^{-1}. This constant c has the same dimension as the ratio $J/[S]$, i.e., initial rate flux divided by the substrate concentration, which is equivalent to the definition of the permeability coefficient P, where $P = J \cdot (C_1 - C_2)^{-1} \cdot A^{-1}$ [38]. Here, J is the net flux, C_1 and C_2 are the substrate concentrations on the two sides of the membrane, and A is the membrane area. Since $c = P \cdot A$, dividing c by the vesicle membrane area gives a Ca^{2+} permeability coefficient, P, of $2 \cdot 10^{-3}$ cm · sec^{-1}. Gunther et al. [16] reported an average permeability of 5 nl · mg^{-1} · sec^{-1} and a permeability coefficient of approximately 10^{-5} cm · sec^{-1} for a number of monovalent cations in rabbit jejunal BBMV. Compared with basal permeabilities (i.e., the permeability in the absence of a specific transport pathway) for a number of nonelectrolytes, as listed by Stein [38], the calculated Ca^{2+} permeability is very high, and is not compatible with a simple diffusion of Ca^{2+}. The identical uptake rates as determined at 0.5 and 5.0 mmol · l^{-1} Ca^{2+} also do not agree with diffusion of Ca^{2+} through a lipid bilayer. Diffusion of Ca^{2+} through a lipid bilayer is energetically unfavorable, due to the hydrophilic nature of the Ca^{2+} ion and, hence, a high degree of hydration. Permeability coefficients of synthetic lipid bilayers for charged molecules are in the range of 10^{-10}–10^{-12} cm · sec^{-1}. A protein-mediated pathway can explain the high Ca^{2+} permeability of the tilapia intestinal brush border membrane. Moreover, the presence of a transporter may form a mechanism to control the steep Ca^{2+} gradient across the brush border membrane, and for its endocrine control.

The nonsaturable component was further analyzed using isotope equilibrium exchange. During the isolation and loading procedure, membrane vesicles were equilibrated in an essentially infinitely large pool of $^{40}Ca^{2+}$, thus allowing masking of the membrane binding sites. The first-order rate constant describing the equilibrium exchange, k, is equal to $J_{max}/(K_m + [S])$ [7]. We found k to be independent of $[S]$, indicating $K_m \gg [S]$ for Ca^{2+} concentrations up to 10 mmol · l^{-1}, so that $k \approx J_{max}/K_m$. The nonsaturable component appears not to be a procedural artifact, but a property of the Ca^{2+} movement across the tilapia intestinal brush border membrane.

The results presented so far lead us to postulate a low-affinity Ca^{2+} transporting mechanism with an allosteric regulatory Ca^{2+} binding site. The mechanism of Ca^{2+} entry across brush border membranes in general is still unknown. The existence of Ca^{2+} channels in brush border membranes has not yet been documented [2]. Wilson et al. [45] found an acceleration of Ca^{2+} transport in rat intestinal BBMV by strontium, and proposed a carrier mechanism for the transport of Ca^{2+}. Based on the observation of many vacuoles in small intestinal enterocytes, Pansu et al. [27] suggested the nonsaturable Ca^{2+} transport in young rats to be pinocytosis-like. However, such a shuttle mechanism for transcellular Ca^{2+} transport cannot, in our opinion, explain the Ca^{2+} permeability found by the same authors in older rats lacking vacuoles in their enterocytes, nor the high Ca^{2+} permeability found in isolated intestinal brush border membranes from tilapia and other animal species.

The results of the equilibrium experiments also permit the conclusion that the tilapia intestine shows no regional differences along the longitudinal axis and the mucosa-serosa axis. Functionally different vesicle subpopulations, e.g., derived from intestinal regions having Ca^{2+} transporters with different kinetic characteristics, would have become visible by nonsuperimposable curves. The homogeneity of the tilapia intestine is in contrast to rat and hamster data, where Ca^{2+} uptake characteristics were different for BBMV preparations from proximal and distal intestinal regions [23, 28, 32]. Stieger and Murer [39] isolated BBMV from rat small intestine by a Mg/EGTA precipitation method, and performed an additional fractionation by free-flow electrophoresis and sucrose density gradient centrifugation. They found different subfractions of BBMV in the whole intestine, as well as in duodenum, ileum and jejunum with respect to enzyme enrichment, transport properties and protein pattern. Brush border membranes from trout middle intestine contain more unsaturated fatty acids, and have a lower sphingomyelin/phosphatidylcholine ratio than membranes from the trout posterior intestine [29]. The differences are undoubtedly important in controlling membrane fluidity and transport properties, and are probably under hormonal control.

Tilapia BBMV did not adjust their volumes to a change in external osmolarity, indicative for a water tightness of the intestinal brush border membrane. In euryhaline fish such as the japanese eel (*Anguilla japonica*) kept in freshwater a high prolactin secretion is correlated with a decreased net water influx, indicating the intestine as a prolactin target [20]. Dave [6] reviews evidence for a prostaglandin-mediated pathway by which prolactin modifies membrane lipid microviscosity. Tilapia enterocytes could well be a target for serum prolactin, explaining the impermeability of BBMV to water.

The authors wish to thank Tom Spanings for his superb organization of fish husbandry, and Maarten de Jong (Dept. of Physiology, Faculty of Medicine, University of Nijmegen) for making the automated stopped-flow apparatus available to us.

References

1. Berg, A. 1968. Studies on the metabolism of calcium and strontium in freshwater fish. I. Relative contribution of direct and intestinal adsorption. *Mem. Ist. Ital. Idrobiol. Dotto Marco de Marchi* **23:**161–169
2. Bronner, F. 1991. Calcium transport across epithelia. *Int. Rev. Cytol.* **131:**169–212
3. Christensen, H.N. 1975. Biological Transport, 2nd ed. pp. 232–246. W.A. Benjamin, London
4. Dacke, C.G. 1979. Calcium Regulation in Submammalian Vertebrates. Academic, London
5. Dahlqvist, A. 1964. Method for assay of intestinal disaccharidases. *Anal. Biochem.* **7:**18–25
6. Dave, J.R. 1986. Prolactin regulation of membrane fluidity and prostaglandin formation. *In:* Actions on Prolactin on Molecular Processes. J.A. Rillema, editor. CRC Press, New York
7. Eilam, Y., Stein, W.D. 1974. Kinetic studies of transport across red blood cell membranes. *In:* Methods in Membrane Biology, Vol. 2. E.D. Korn, editor. Plenum, New York
8. Fenwick, J.C. 1989. Calcium exchange across fish gills. *In:* Vertebrate Endocrinology. Fundamentals and Biomedical Implications. Vol. III. P.K.T. Pang, M.P. Schreibman, editors. pp. 319–342. Academic, New York
9. Fishman, W.H., Bernfeld, P. 1955. Glucuronidases. *Meth. Enzymol.* **1:**262–269
10. Flik, G., Fenwick, J.C., Kolar, Z., Mayer-Gostan, N., Wendelaar Bonga, S.E. 1986. Effects of low ambient calcium levels on whole-body Ca^{2+} flux rates and internal calcium pools in the freshwater cichlid teleost, *Oreochromis mossambicus*. *J. Exp. Biol.* **120:**249–264
11. Flik, G., Schoenmakers, Th.J.M., Groot, J.A., Van Os, C.H., Wendelaar Bonga, S.E. 1990. Calcium absorption by fish intestine: the involvement of ATP- and sodium-dependent calcium extrusion mechanisms. *J. Membrane Biol.* **113:**13–22
12. Flik, G., Van Rijs, J.H., Wendelaar Bonga, S.E. 1985. Evidence for high-affinity Ca^{2+}-ATPase activity and ATP-driven Ca^{2+}-transport in membrane preparations of the gill epithelium of the cichlid fish *Oreochromis mossambicus*. *J. Exp. Biol.* **119:**335–347
13. Flik, G., Wendelaar Bonga, S.E., Fenwick, J.C. 1985. Active Ca^{2+} transport in plasma membranes of branchial epithelium of the North-American eel, *Anguilla rostrata* LeSueur. *Biol. Cell* **55:**265–272
14. Ghijsen, W.E.J.M., Ganguli, U., Stange, G., Gmaj, P., Murer, H. 1987. Calcium uptake into rat small intestinal brush border membrane vesicles: characterization of transmembrane calcium transport at short initial incubation times. *Cell Calcium* **8:**157–169
15. Ghishan, F.K., Arab, N., Nylander, W. 1989. Characterization of calcium uptake by brush border membrane vesicles of human small intestine. *Gastroenterology* **96:**122–129
16. Gunther, R.D., Schell, R.E., Wright, E.M. 1983. Ion permeability of rabbit intestinal brush border membrane vesicles. *J. Membrane Biol.* **78:**119–127
17. Haase, W., Schäfer, A., Murer, H., Kinne, R. 1978. Studies on the orientation of brush-border membrane vesicles. *Biochem. J.* **172:**57–62
18. Hennessen, U., Drüeke, T., Comte, L., Steuf, M.C., McCarron, D.A., Lacour, B. 1990. Calcium uptake kinetics into brush-border membrane vesicles: higher V_{max} in the spontaneously hypertensive rat than in normotensive control. *Biochem. Biophys. Res. Comm.* **170:**742–747
19. Hirano, T. 1989. The corpuscles of Stannius. *In:* Vertebrate Endocrinology. Fundamentals and Biomedical Implications. Vol. III. P.K.T. Pang, M.P. Schreibman, editors. pp. 139–169. Academic, New York
20. Hirano, T., Morisawa, M., Ando, M., Utida, S. 1976. Adaptive changes in ion and water transport mechanism in the eel intestine. *In:* Intestinal Ion Transport. Proceedings of the International Symposium on Intestinal Ion Transport held at Titisee in May 1975. J.W.L. Robinson, editor. pp. 301–317. MTP Press Ltd., UK
21. Hopfer, U. 1981. Kinetic criteria for carrier-mediated transport mechanisms in membrane vesicles. *Fed. Proc.* **40:**2480–2485
22. Ichii, T., Mugiya, Y. 1983. Effects of a dietary deficiency in calcium on growth and calcium uptake from the aquatic environment in the goldfish, *Carassius auratus*. *Comp. Biochem. Physiol.* **74A:**259–262
23. Iskandarani, M., Miller, D.L., Schedl, H.P. 1981. Kinetics of calcium transport in the hamster duodenum and ileum. *Gastroenterology* **81:**903–909
24. Leatherbarrow, R.J. 1987. A non-linear regression data analysis program for the IBM PC. Elsevier Biosoft, Amsterdam
25. Mayer-Gostan, N., Bornancin, M., DeRenzis, G., Naon, R., Yee, J.A., Shew, R.L., Pang, P.K.T. 1983. Extraintestinal calcium uptake in the killifish, *Fundulus heteroclitus*. *J. Exp. Zool.* **227:**329–338
26. Miller, A., III, Bronner, F. 1981. Calcium uptake in isolated brush-border vesicles from rat small intestine. *Biochem. J.* **196:**391–401
27. Pansu, D., Bellaton, C., Bronner, F. 1983a. Developmental changes in the mechanisms of duodenal calcium transport in the rat. *Am. J. Physiol.* **244:**G20–G26
28. Pansu, D., Bellaton, C., Roche, C., Bronner, F. 1983. Duodenal and ileal calcium absorption in the rat and effects of vitamin D. *Am. J. Physiol.* **244:**G695–G700
29. Pelletier, X., Duportail, G., Leray, C. 1986. Isolation and characterization of brush-border membranes from trout intestine. Regional differences. *Biochim. Biophys. Acta* **856:**267–273
30. Perry, S.F., Wood, C.M. 1985. Kinetics of branchial calcium uptake in the rainbow trout: effects of acclimation to various external calcium levels. *J. Exp. Biol.* **116:**411–433
31. Rasmussen, H., Fontaine, O., Max, E.E., Goodman, D.B.P. 1979. The effect of 1α-hydroxyvitamin D_3 administration on calcium transport in chick intestine brush border membrane vesicles. *J. Biol. Chem.* **254:**2993–2999
32. Schedl, H.P., Wilson, H.D. 1985. Calcium uptake by intestinal brush border membrane vesicles. Comparison with *in vivo* calcium transport. *J. Clin. Invest.* **76:**1871–1878
33. Schedl, H.P., Wilson, H.D., Mathur, S.N., Murthy, S., Field, F.J. 1989. Effects of phospholipid or cholesterol enrichment of rat intestinal brush border membrane on membrane order and transport of calcium. *Metabolism* **38:**1164–1169
34. Schoenmakers, Th.J.M., Klaren, P.H.M., Flik, G., Pang, P.K.T., Wendelaar Bonga, S.E. 1992. Actions of cadmium

on basolateral plasma membrane proteins involved in calcium uptake by fish intestine. *J. Membrane Biol.* **127:**161–172

35. Schoenmakers, Th.J.M., Visser, G.J., Flik, G., Theuvenet, A.P.R. 1992. CHELATOR: an improved method for computing metal ion concentrations in physiological solutions. *Biotechniques* **12:**870–879
36. Sillén, L.G., Martell, A.E. 1964. Stability constants of metal ion complexes. The Chemical Society, Special Publication no. 17, London
37. Steck, T.L., Kant, J.A. 1974. Preparation of impermeable ghosts and inside-out vesicles from human erythrocyte membranes. *Meth. Enzymol.* **31A:**172–180
38. Stein, W.D. 1986. Transport and Diffusion across Cell Membranes. Academic, Orlando
39. Stieger, B., Murer, H. 1983. Heterogeneity of brush-border-membrane vesicles from rat small intestine prepared by a precipitation method using Mg/EGTA. *Eur. J. Biochem.* **135:**95–101
40. Tacnet, F., Watkins, D.W., Ripoche, P. 1990. Studies of zinc transport into brush border membrane vesicles isolated from pig small intestine. *Biochim. Biophys. Acta* **1024:**323–330
41. Taylor, C.W. 1985. Calcium regulation in vertebrates: an overview. *Comp. Biochem. Physiol.* **82A:**249–255
42. Titus, E., Karasov, W.H., Ahearn, G.A. 1991. Dietary modulation of intestinal nutrient transport in the teleost fish tilapia. *Am. J. Physiol.* **261:**R1568–R1574
43. Van Os, C.H. 1987. Transcellular calcium transport in intestinal and renal epithelial cells. *Biochim. Biophys. Acta* **906:**195–222
44. Wendelaar Bonga, S.E., Pang, P.K.T. 1991. Control of calcium regulating hormones in the vertebrates: parathyroid hormone, calcitonin, prolactin and stanniocalcin. *Int. Rev. Cytol.* **128:**139–213
45. Wilson, H.D., Schedl, H.P., Christensen, K. 1989. Calcium uptake by brush-border membrane vesicles from the rat intestine. *Am. J. Physiol.* **257:**F446–F453

Received 10 July 1992; revised 2 October 1992